A NUMERICAL STUDY OF TURBULENT FLOW USING A NONSTAGGERED MESH

Mohamed Agouzoul, Marcelo Reggio,
and Ricardo Camarero

EPM/RT-86-44

(1986)

EPM/RT-86-44

A NUMERICAL STUDY OF TURBULENT FLOW USING A NONSTAGGERED MESH

Mohamed Agouzoul, Marcelo Reggio,

and Ricardo Camarero

Ecole Polytechnique de Montréal

octobre 1986

This work was carried out with the financial support of NSERC of Canada and the Ministère de l'Education Nationale du Maroc

Dêpot légal , 4e trimestre 1986
Blibliothèque nationale du Québec
Blibliothèque nationale du Canada

Pour se procurer une copie de ce document, s'adresser au:

Service de l'édition
Ecole Polytechnique de Montréal
Case Postale 6079, Succ. "A"
Montréal,Québec H3C 3A7
(514) 340-4903

Compter 0,05$ par page(arrondir au dollar le plus près),plus 1,50$(Canada) ou 2,50$(étranger) pour la couverture,les frais de poste et la manutention.Régler en dollars canadiens par chèque ou mandat-poste au nom de l'Ecole Polytechnique de Montréal.Nous n'honorerons que les commandes accompagnées d'un paiement,sauf s'il y a eu entente préalable, dans le cas d'établissements d'enseignement ou d'organismes canadiens.

ABSTRACT

A calculation scheme to predict incompressible turbulent flows in arbitrary shapes is presented. The procedure is based on the solution of the primitive-variable formulation of the time dependent Reynolds averaged Navier-Stokes equations in general curvilinear coordinates. An ordinary computational cell is used for continuity and transport balances; and all the physical properties are stored at the center of this calculation element. The scheme, use an overlapping mesh along with forward and backward differencing for mass and pressure gradients respectively. This procedure prevents in a different manner than the staggered grid approach, the oscillatory behaviour of the pressure field. The employed methodology follows a former practice used to the solution of laminar flows. The $k-\varepsilon$ model is used to describe the turbulent flow process. Particular attention is given to the boundary condition for the turbulent properties. The method used here is easily extended to three dimensions. Computed results are compared with numerical and experimental data.

NOMENCLATURE

C	Chord
C_p	pressure coefficient
C_1, C_2, C_d	constants in turbulence model
E_*	constant for the law of the wall
E, F	flux vectors in ξ and η coordinate directions
g^{ij}	metric tensor components
G	rate of production of the turbulence kinetic energy
J	Jacobian of transformation matrix
k	turbulence kinetic energy
L	spacing between plates
p	pressure
p^*	estimated pressure
q	vector of conservation variables
r	radial distance
r_i	inner radius of expanding duct
R, S	viscous flux terms in ξ and η coordinate directions
R_e	Reynolds number
t	time
T	source term in the transport equations
u, v	time-averaged velocity components in x and y directions
u_*	friction velocity
U, V	time-averaged contravariant velocity components in ξ and η directions
U^*, V^*	tentative curvilinear velocity components
x, y	Cartesian coordinates
y_p	conventional normal distance to the wall
ξ, η	curvilinear coordinates

δp	pressure correction
Δt	time step
$\delta U, \delta V$	contravariant velocity corrections
α	geometric index, $\alpha=0$, two dimensions: $\alpha=1$, axisymmetry
ε	turbulence energy dissipation
κ	the von Karman constant
ν	kinematic viscosity
ν_e	effective viscosity
ν_t	turbulent viscosity
$\sigma_k, \sigma_\varepsilon$	turbulent Prandtl numbers

Subscripts

c	centerline
p	refers to the grid node next to the wall
x, y ξ, η	first partial differentiation
i, j	variable location
0	reference value

INTRODUCTION:

Over the last two decades the simulation of numerous incompressible fluid flow problems has been carried out by explicit time-dependent algorithms which solve the primitive variable form of the Navier-Stokes equations. Many of these procedures use a finite-volume method with a staggered grid[1] arrangement, which by its intrinsic nature, requires a different location for the pressure and velocity components.

In order to alleviate the geometric complexities of such classical discretization, an alternative approach has been employed in Ref.[2] for the solution of laminar flows. In this technique the pressure and velocity components are located at a common point, and the same basic element is used for both the continuity and momentum balances. To avoid the delicate problem of unrealistic fields arising with such discretization, an opposed difference scheme for pressure and momentum fluxes in the main flow direction, coupled with an overlapping mesh in the secondary direction is applied

In the present study these ideas are applied to the solution of turbulent flows in arbitrary geometries. The scheme is incorporated into the solution of the time dependent Reynolds averaged Navier-Stokes equations closed with the two additional equations of the $k-\varepsilon$ model. All the variables (velocity components, pressure, turbulence kinetic energy, and turbulence energy dissipation) are stored at the center of the same computational cell which is used for all balances. The required domain discretization is carried out by the

use of a grid which is numerically generated by the body-fitted technique[3,4]. The governing transport equations are then formulated for a general curvilinear coordinate system in which the Cartesian velocity components appear as dependent variables, leading to the conservation form.

A characteristic aspect of the computation of incompressible flows, is presented by the extraction of a pressure field which drives velocities that respect both mass and momentum equations simultaneously. This p-v coupling problem is solved by using a simple but effective procedure, which is established by combining the continuity and momentum equations in a way similar to that proposed by the SIMPLE[5] method, and modified for a curvilinear mesh.

An alternative approach to the more standard "slip-velocity" is used for the treatment of the wall boundary condition. The present method takes into account the variations of the velocity in the next-wall region, by using an" equivalent viscosity" together with the real zero velocity condition. This procedure which does not require the direction of the velocity at the first node near the wall, allows a simple extrapolation to three-dimensional problems.

2. TRANSPORT EQUATIONS

The unsteady, incompressible, turbulent flow is governed by

the Reynolds averaged Navier-stokes equations. Using the eddy viscosity concept[6] along with the closure k-ε model, these equations can be written in Cartesian and/or axisymmetric form as follows.

Continuity:

$$\frac{\partial}{\partial x}(r^{\alpha}u) + \frac{\partial}{\partial y}(r^{\alpha}v) = 0 \qquad (1)$$

x-momemtum:

$$\frac{\partial u}{\partial t} + \frac{1}{r^{\alpha}}\frac{\partial}{\partial x}(r^{\alpha}u^{2}) + \frac{1}{r^{\alpha}}\frac{\partial}{\partial y}(r^{\alpha}uv) =$$

$$-\frac{\partial p}{\partial x} + \frac{1}{r^{\alpha}}\frac{\partial}{\partial x}(2r^{\alpha}\nu_{e}\frac{\partial u}{\partial x}) + \frac{1}{r^{\alpha}}\frac{\partial}{\partial y}(r^{\alpha}\nu_{e}(\frac{\partial u}{\partial y} + \frac{\partial v}{\partial x})) \qquad (2)$$

y-momemtum:

$$\frac{\partial v}{\partial t} + \frac{1}{r^{\alpha}}\frac{\partial}{\partial x}(r^{\alpha}uv) + \frac{1}{r^{\alpha}}\frac{\partial}{\partial y}(r^{\alpha}v^{2}) =$$

$$-\frac{\partial p}{\partial y} + \frac{1}{r^{\alpha}}\frac{\partial}{\partial x}(r^{\alpha}\nu_{e}(\frac{\partial v}{\partial x} + \frac{\partial u}{\partial y})) + \frac{1\cdot\partial}{r^{\alpha}\partial y}(2r^{\alpha}\nu_{e}\frac{\partial v}{\partial y}) - \alpha\nu_{e}\frac{2v}{r^{2}} \qquad (3)$$

Turbulence kinetic energy:

$$\frac{\partial k}{\partial t} + \frac{1}{r^{\alpha}}\frac{\partial}{\partial x}(r^{\alpha}uk) + \frac{1}{r^{\alpha}}\frac{\partial}{\partial y}(r^{\alpha}vk) =$$

$$\frac{1}{r^{\alpha}}\frac{\partial}{\partial x}(r^{\alpha}\frac{\nu_{t}}{\sigma_{k}}\frac{\partial k}{\partial x}) + \frac{1}{r^{\alpha}}\frac{\partial}{\partial y}(r^{\alpha}\frac{\nu_{t}}{\sigma_{k}}\frac{\partial k}{\partial y}) + \nu_{t}G - \varepsilon \qquad (4)$$

Turbulence dissipation rate:

$$\frac{\partial \varepsilon}{\partial t} + \frac{1}{r^{\alpha}}\frac{\partial}{\partial x}(r^{\alpha} u \varepsilon) + \frac{1}{r^{\alpha}}\frac{\partial}{\partial y}(r^{\alpha} v \varepsilon) =$$

$$\frac{1}{r^{\alpha}}\frac{\partial}{\partial x}\left(r^{\alpha}\frac{\nu_t}{\sigma_{\varepsilon}}\frac{\partial \varepsilon}{\partial x}\right) + \frac{1}{r^{\alpha}}\frac{\partial}{\partial y}\left(r^{\alpha}\frac{\nu_t}{\sigma_{\varepsilon}}\frac{\partial \varepsilon}{\partial y}\right) + \nu_t C_1 \frac{\varepsilon}{k} G - C_2 \frac{\varepsilon^2}{k} \qquad (5)$$

where the effective viscosity ν_m appearing in the momentum transport equations is given by:

$$\nu_m = \nu_t + 1/R_m \qquad (6)$$

in which $1/R_m$ represents the dimensionless molecular viscosity, and ν_t the dimensionless turbulent viscosity calculated by the relation:

$$\nu_t = C_d \, k^2/\varepsilon \qquad (7)$$

The source term G appearing in the k-ε equations is given by the following expression:

$$G = 2\left[\left(\frac{\partial u}{\partial x}\right)^2 + \left(\frac{\partial v}{\partial y}\right)^2 + \alpha\frac{v^2}{r^2}\right] + \left(\frac{\partial u}{\partial y} + \frac{\partial v}{\partial x}\right)^2 \qquad (8)$$

The value of the five empirical constants appearing in the above equations are[7]:

$C_1 = 1.44$ $\quad C_2 = 1.92$ $\quad \sigma_k = 1.$ $\quad \sigma_{\varepsilon} = 1.3$ $\quad C_d = 0.09$

Finally the symbol α represents a geometric index to denote axisymmetry (α=1) or two dimensional (α=0) configurations. In the axisymetric case y is equivalent to the radius r.

Transformed Equations

The set of conservation equations are formulated for a curvilinear coordinate system with Cartesian velocity components taken as the dependent variables, in this manner the transformed governing equations can be written in the strong conservative form [8]. In the axisymmetric case, because the use of a cylindrical reference system, the radial momemtum equation presents an inevitable source term, and this can only be written in the semi-strong form.

Following this approach, Eqs. (1) to (5) can be written in generalized coordinates, ξ and η, as:

$$\frac{\partial q}{\partial t} + \frac{\partial E}{\partial \xi} + \frac{\partial F}{\partial \eta} = \frac{\partial R}{\partial \xi} + \frac{\partial S}{\partial \eta} + T \qquad (9)$$

where:

$$q = Jr \begin{bmatrix} 0 \\ u \\ v \\ k \\ \varepsilon \end{bmatrix} \qquad E = Jr^{\alpha} \begin{bmatrix} U \\ uU + p\xi_x \\ vU + p\xi_y \\ kU \\ \varepsilon U \end{bmatrix} \qquad F = Jr^{\alpha} \begin{bmatrix} V \\ uV + p\eta_x \\ vV + p\eta_y \\ kV \\ \varepsilon V \end{bmatrix}$$

$$R = Jr^{\alpha}\nu_{\infty} \begin{bmatrix} 0 \\ g^{11}u_{\xi} + g^{12}u_{\eta} + \xi_x u_{\xi} + \xi_x\eta_x u_{\eta} + \xi_x\xi_y v_{\xi} + \xi_y\eta_x v_{\eta} \\ g^{11}v_{\xi} + g^{12}v_{\eta} + \xi_y v_{\xi} + \xi_y\eta_y v_{\eta} + \xi_x\xi_y u_{\xi} + \xi_x\eta_y u_{\eta} \\ (g^{11}k_{\xi} + g^{12}k_{\eta})/\sigma_k \\ (g^{11}\varepsilon_{\xi} + g^{12}\varepsilon_{\eta})/\sigma_{\varepsilon} \end{bmatrix}$$

$$S = Jr^{\alpha}\nu_{\infty} \begin{bmatrix} 0 \\ g^{21}u_{\xi} + g^{22}u_{\eta} + \eta_x\xi_x u_{\xi} + \eta_x u_{\eta} + \eta_y\xi_x v_{\xi} + \eta_y\eta_x v_{\eta} \\ g^{21}v_{\xi} + g^{22}v_{\eta} + \eta_y\xi_y v_{\xi} + \eta_y v_{\eta} + \eta_x\xi_y u_{\xi} + \eta_y\eta_x u_{\eta} \\ (g^{12}k_{\xi} + g^{22}k_{\eta})/\sigma_k \\ (g^{12}\varepsilon_{\xi} + g^{22}\varepsilon_{\eta})/\sigma_{\varepsilon} \end{bmatrix}$$

$$T = Jr^{\alpha}\nu_{\infty} \begin{bmatrix} 0 \\ 0 \\ (p - \nu_{\infty}2v/R)\alpha \\ \nu_{\infty}G_{\kappa} - \varepsilon \\ \nu_{\infty}C_1 G_{\kappa}\varepsilon/k - C_2\varepsilon\tilde{\varepsilon}/k \end{bmatrix}$$

and:

$$G_{**} = 2((\xi_x u_\xi + \eta_x u_\eta)^2 + (\xi_y v_\xi + \eta_y v_\eta)^2 + \alpha v^2/r^2)) + (\xi_x u_\xi + \eta_y u_\eta + \xi_x v_\xi + \eta_x v_\eta)^2$$

The curvilinear velocity components U,V and the Cartesian velocity components u,v are related by:

$$U = u\xi_x + v\xi_y$$
$$V = u\eta_x + v\eta_y \qquad (10)$$

The expressions for the metric terms $\xi_x, \xi_y, \eta_x, \eta_y$, the jacobian J and the contravariant metric tensor components g^{11}, g^{12}, g^{21}, and g^{22} are given by:

$$\xi_x = y_\eta/J, \qquad \xi_y = -x_\eta/J$$

$$\eta_x = -y_\xi/J, \qquad \eta_y = x_\xi/J$$

$$J = x_\xi y_\eta - x_\eta y_\xi$$

$$g^{11} = \xi_x^2 + \xi_y^2 \qquad g^{12} = \xi_x\eta_x + \xi_y\eta_y$$

$$g^{21} = g^{12} \qquad g^{22} = \eta_x^2 + \eta_y^2$$

3. NUMERICAL DISCRETIZATION

The governing equations are solved using a conservative control-volume approach. The discrete form of such system is derived by integrating these equations locally over these finite volumes. A nonstaggered mesh[2], previously derived for the solution of laminar flows is employed here to predict the turbulent counterpart.

There are several ways of representing the temporal and spatial derivatives of the source equations in discrete form. The temporal differencing adopted here is explicit, and in compact form can be written as:

$$\Delta q + \Delta t(E_\xi + F_\eta)^n = \Delta t(R_\xi + S_\eta + T)^n \qquad (11)$$

where Δ denotes the forward time difference operator and n the time level .

In the computational grid used in this study, the velocity

components u,v, the pressure p, the turbulence kinetic energy k and the turbulence dissiption rate ε, are stored at the node (i+1/2,j) of the computational element illustrated in Fig. 1.

The spatial discretization requires the knowledge of the mass flow, pressure, convected properties, and diffusion term at the element faces. First, attention is turned on the mass flow and pressure evaluation.

As a result of the overlapping procedure in the j direction, the working variables(with the exception of the pressure which is interpolated) are known at the i+1/2,j+1, and i+1/2,j-1 stations. Consequently, the mass flow represented by the curvilinear velocity components U and V can be directly obtained by applying the discrete equivalent of relations (10).

On the other hand, the inspection on the "streamwise" or logical i direction, reveals that velocities and pressure are not available at the i,j and i+1,j locations. This time, the opposed differencing technique will be employed to calculate the required mass and pressure gradients. In particular, mass differencing is obtained via upwinding, while pressure differencing is computed through downwinding. That means for example, that the flux across the i face is controlled by the velocity at the station i-1/2,j; in the same manner, the pressure acting on the i face can be considered as the one located at the i+1/2,j node.

The discrete form of the momentum and turbulence equations also requires the computation of convected variables and diffussion terms at the cell faces. These spatial variations are approximated by using the weighted upstream scheme of Raithby and Torrance [9].

As mentionned earlier, the central idea in the present solution algorithm is an extension to turbulent flows of the methodology used in Ref[2]; it follows standard practice, so only a general description will be given here.

The iteration sequence is as follows:

- Pressure, Cartesian and corresponding curvilinear velocity components, k, and ε fields are guessed.
- The x-momemtum, y-momentum ,turbulent kinetic energy and dissipation rate transport equations are solved.
- Pressure and curvilinear velocity corrections δp and δU, δV respectively, are calculated and introduced to ensure that the continuity equation is respected These paramaters are added to the existing fields as:

$$U=U^*+\delta U$$
$$V=V^*+\delta V \qquad (12)$$
$$p=p^*+\delta p$$

where the superscript star is used here to denote intermediate estimates which do not satisfy mass conservation.

- The modification described by Eq.12 is done point-by-point in the inlet-outlet direction. This procedure is repeated until the mass source level fall below a predetermined limit of accuracy.
- The Cartesian velocity components are decoded from curvilinear components and the boundary conditions applied or calculated for the turbulence kinetic energy and dissipation rate, k and ε respectively.
- The effective viscosities are evaluated using the new mean velocity, turbulent kinetic energy, and dissipation rate fields.
- The time level is advanced and the cycle repeated until the steady state is reached.

4. BOUNDARY CONDITIONS

The two-equation k-ε model is only valid for fully turbulent regions, and does not include the viscous sublayer effects. To take account of these phenomena, and without using a large number of grid points near the wall, the alternative technique known as the "wall function" method is adopted. Following this approach the boundary conditions are derived from the velocity profile at the first node away from the wall .

Usually, to get a better approximation for the shear stresses acting on the wall-adjacent elements, an imaginary wall slip velocity is used instead of the no slip velocity condition. However, this proven methodology becomes complicated for the calculation of

three-dimensional flows(see for example Ref[10]), because it requires the direction of the velocity at the first node near the wall. In the present effort, an alternative approach[11] which only needs the value and not the direction of the velocity at such station, is employed.

The basic idea under this treatment lies in using an hypothetical or "equivalent viscosity" to replace the actual viscosity, so as to account for the non-linearity of the velocity, consequently to evaluate the shear force in the discrete representation of the momentum balances of the wall-adjacents elements. This "equivalent viscosity" idea, which is applied jointly with the physical no-slip condition, allows a rather straight-forward extension to the computation of three dimensional flows

Attention is now focussed on the calculation and implementation of the required properties next to the wall. For this, two different situations are distinguished.

First, if the node next to the wall is outside the laminar sublayer, i.e when the value of the dimensionless distance defined as $y_p^+ = y_p\ u_*/\nu$ is greater than 30; the following wall function[12] is used:

$$\frac{u_p}{u_*} = \frac{1}{\chi} \ln(E_* y_p u_*/\nu) \qquad (13)$$

where u_p represents the velocity component parallel to boundary at the first node next to the wall; χ and E_* are constant from the law wall, and y_p is the distance normal to the wall.

From the above equation and by a Newton-Raphson method, the friction velocity u_* is iteratively calculated. The values of the k-ε turbulence properties at the first node away from the wall indicated by the subscript p, are then specified through the following relationships:

$$k_p = u_*^2/\sqrt{C_\mu} \qquad (14)$$

$$\varepsilon_p = u_*^3/\kappa y_p \qquad (15)$$

These values are used as the boundary condition for the next time level n+1, together with an updated "equivalent-viscosity" calculated via:

$$\nu_{eff} = \frac{\kappa\, y_p\, u_*}{\ln(E_*\, y_p\, u_*/\nu)} \qquad (16)$$

In the second case, when the node next to the wall is inside the laminar sublayer; the friction velocity u_* is calculated from:

$$\frac{u_p}{u_*} = \frac{y_p u_*}{\nu} \qquad (17)$$

which represents the velocity variation in this region. This time relations (14) and (15) are also used to update k and ε at the first nodes.However the shear force is evaluated by using the laminar viscosity, instead of the "equivalent-viscosity".

At the inlet the distribution of the turbulence kinetic energy and the dissipation of the turbulence energy is estimated; these values are based on acquired experience; except at the nodes near the wall, where they are calculated from the inlet velocity profile and the wall function.(Eqns. 13, 14, and 15)

At the exit all the properties are extrapolated by assuming a fully developed flow .

COMPUTED RESULTS

Parallel-walled channel.

To evaluate the present scheme the developing flow between parallel plates was attempted. Calculations were made on a channel with a length-to-width ratio of 60, and for a Reynolds number of 192,000. The discretization was carried out by using a 17x180 grid. At the inlet uniform velocity, and constant turbulence kinetic energy and dissipation rate are prescribed.

The computed values for the center-line velocity, together with the experimental and numerical results of Refs.[13] and [14] represented by dots and dashed line respectively, are displayed in Fig.2a. Although the velocity peak in the calculated solution appearing at an early stage of the development, around x=25d, slighty underestimates the value of the velocity shown by the other data, the overall agreement seems to be reasonable, if one considers that the large velocity scale exaggerates the differences.

The predicted developed velocity profile ,normalized in terms of the centerline velocity is plotted along the experimental data of Ref[15] in Fig.2b. Inspection of this figure shows that the present predictions are in good agreement with the measurements.

Axisymmetric Diffuser.

The next problem studied was that of the turbulent flow in a diffuser. The geometrical configuration for this case was chosen after a test case investigated by Habib[16], which consists on a diffuser with a 20° half angle. Calculations were made for a node distibution of 51x31 and for R_e= 20,000.

Fig. 3a depicts the calculated velocity field and axial mean velocity contours. The general trend of this latter are in good agreement with the results presented by Ref.[16]. Fig.3b illustrates the calculated streamlines, where the recirculation zone is clearly evident; the magnitude and location of this region confirm the numerical predictions of Habib[16].

Calculations of the mean flow velocity at three axial stations; namely at x/r=3.2, x/r=6.4 , and x/r=12.2, are compared with the measuremets of Ref[16]. Observation on the calculated mean velocities, as shown in Fig. 3c, reveals that these are in concordance with the experiment apart from small discrepancies, particulary near the right boundary of the recirculation zone (x/r=6.4). As indicated by the above reference, which found a similar situation when comparing

his numerical and experimental results, this can be attributed, at least in part, to rectification of the hot-wire signal in regions of low mean velocity. Further downstream, the discrepancy between the measurements and calculations decrease.

NACA 0012 Cascade.

As a preliminary effort to turbomachinery flow analysis, a NACA0012 cascade at zero degree angle of attack (i.e. without separation) was considered. The chord-to-pitch ratio was of 2 and the front and rear boundaries were located at one chord lengths away form the leading and trailing edges. The Reynolds number employed in the calculation was of 20,000. The whole domain covering periodic and solid wall zones, was discretized with a 21x53 grid

The surface pressure distribution is plotted in Fig 4 and compared with the experimental data of Gregory and O'Reilly[17]. In general the pressure distribution shows good agreement with the measurements. The minimun value of the pressure is well predicted; however its position is sligthy downstream compared to the experimemtal data. Small discrepancies are shown after the cascade throat towards the trailing edge as presented by an estimated lower pressure near such region. These differences can be attributed to a unsufficiently fine grid spacing in the trailing edge vicinity to resolve the important gradients in that zone.

CONCLUSIONS

A calculation algorithm for turbulent flows, which employs an explicit temporal differencing, a nonstaggered mesh along with weighted upwind/central and opposed spatial discretization, has been implemented. The method is based on the finite-volume solution of the governing equations in curvilinear coordinates. These are generated numerically by the use of the body-fitted technique. A conservative form of the Reynolds averaged Navier-Stokes equations has been developed and applied; and a particular treatement of the wall boundary conditions through the "equivalent-viscosity" idea has been employed. The resulting procedure was applied to the computation of plane, recirculating axisymmetric, and cascade flows. Comparisons on the obtained results and available numerical and experimental data show that the flow behaviour can reasonably well predicted for the nonsepareted and recirculating cases. It remains to be seen in a further development, what additional difficulties may arrive on the calculation of three-dimensional flows

ACKNOWLEDGEMENTS.

The support of this work by the Natural Science and Engineering Research Council of Canada (NSERC) is gratefully acknowledged.

REFERENCES

1. Harlow, F. H. and Welch, J. E. " Numerical calculation of time-dependent viscous incompressible flow of fluid with free surface", Phys. Fluids, Vol. 8, No. 12 , pp. 2182-2189, 1965

2. Reggio, M. and Camarero, R. "Numerical solution procedure for viscous incompressible flows", Numerical Heat Transfer, vol 10, 1986.

3. Thompson J.F, Thames F.C and Mastin C.W, "Automatic numerical generation of body-fitted curvilinear coordinates for fields containing any number of arbitrary two-dimensional bodies", Journal of Computational Physics, vol 15,p.229, 1984

4. Camarero, R. et al "Introduction to grid generation in turbomachinery, VKI lecture Serie 2 , Numerical techniques for viscous calculations in turbomachinery Jan. 20-24 ,1986

5 .Patankar S.V. Numerical Heat Transfer and Fluid Flow, Hemisphere Publishing Corporation, Washington, 1980

6. Boussinesq ,J., "Theorie de l'ecoulement tourbillonnant ", Mem. Pre. Par. Div. Sav. 23, paris (1877)

7. Launder ,B. E. and Spalding D. B. " Lectures in mathematical models of turbulence " , Academic Press, London(1972)

8. Agouzoul, M. ,Reggio, M., Camarero, R. " A note on the conservation

form of the Reynolds-averaged Navier-Stokes equations in generalized coordinates, submitted to AIAA.

9. Raithby, G.D. and Torrance, K.E. "Upstream-weighted differencing schemes and their application to elliptic problems involving fluid flow " Computer Fluids Vol. 2, pp 191-206 1974

10. El Dib, I. " Numerical Calculation of Internal Flows with Curvature", Ph.D Thesis, Northwestern University, 1985.

11. Nakayama, A. " Three-dimensional flow within conduits of arbitrary geometrical configurations",Ph.D Thesis, University of Illinois at Urbana-Champaign, 1981.

12. Launder, B.E. and Spalding, D.B., "The numerical calculation of turbulent flows", Computer Methods in Applied Mechanics and Engineering, Vol 3, No.2 ,pp.269-289, 1974

13. Bradshaw, P, Dean, R.B and McEligott D.M "Calculation of interacting turbulent shear layers: duct flow", J. Fluid Engng. 95(2), p.214, 1973

14. Stephenson P.L., "A theoretical study of heat transfer in two-dimensional turbulent flow in a circular pipe and between parallel and diverging plates", Int. J. Heat Mass Transfer., Vol 19, pp.413-423, 1976.

15. Schilichting H. "Boundary Layer Theory, McGraw-Hill Company, 1960

16. Habib, M.A. and Whitelaw, J.H. "The Calculation of Turbulent Flow in wide-angle diffusers" Numerical Heat Transfer, Vol. 5, pp.145-164, 1982.

17. Gregory, N. and O'Reilly, C. L., "Low Speed Aerodynamic Characteristics of NACA 0012 Airofoil Section , Including the Effects of Upper Surface Roughness Simulation Hoarfrost ," National Physical Laboratory, Teddington , England, Aero Repot. 1308, 1970.

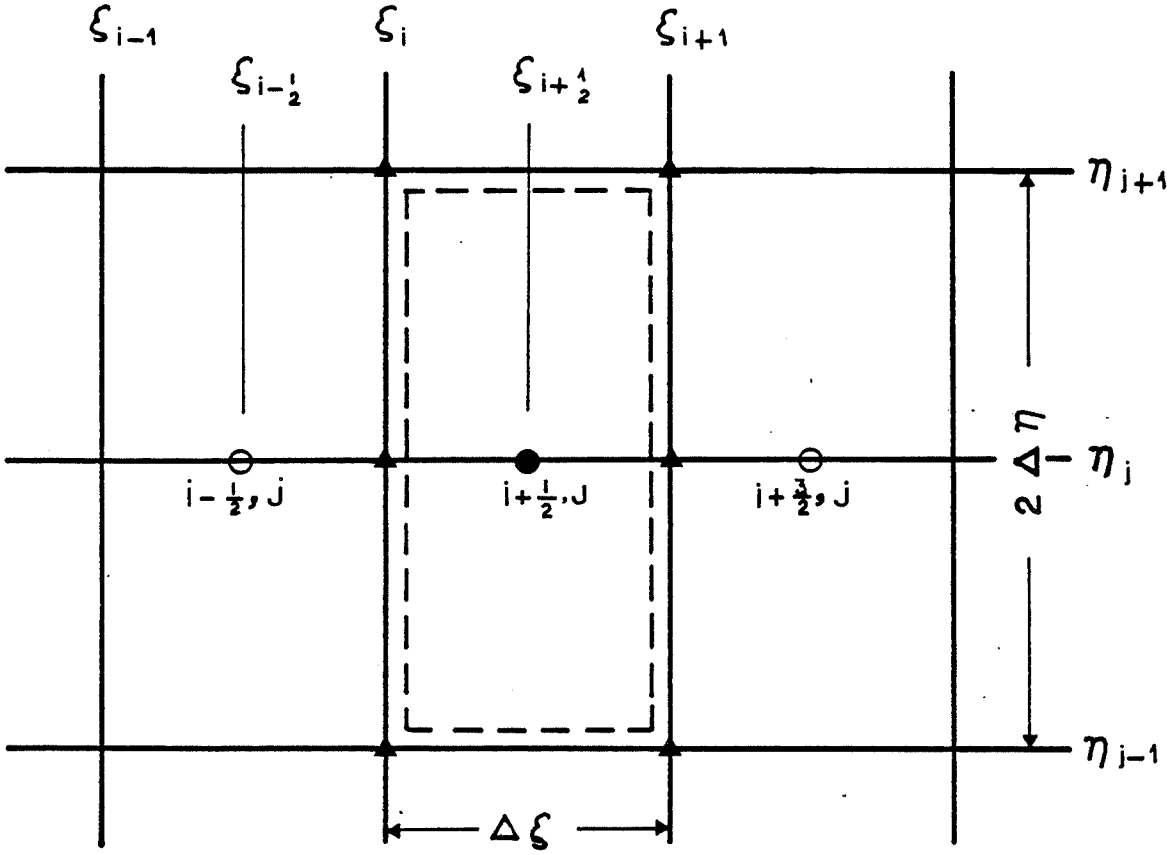
ξ_{i-1}
ξ_i
ξ_{i+1}
$\xi_{i-\frac{1}{2}}$
$\xi_{i+\frac{1}{2}}$
η_{j+1}
η_j
η_{j-1}
$2\Delta\eta$
$i-\frac{1}{2}, j$
$i+\frac{1}{2}, J$
$i+\frac{3}{2}, j$
$\Delta\xi$

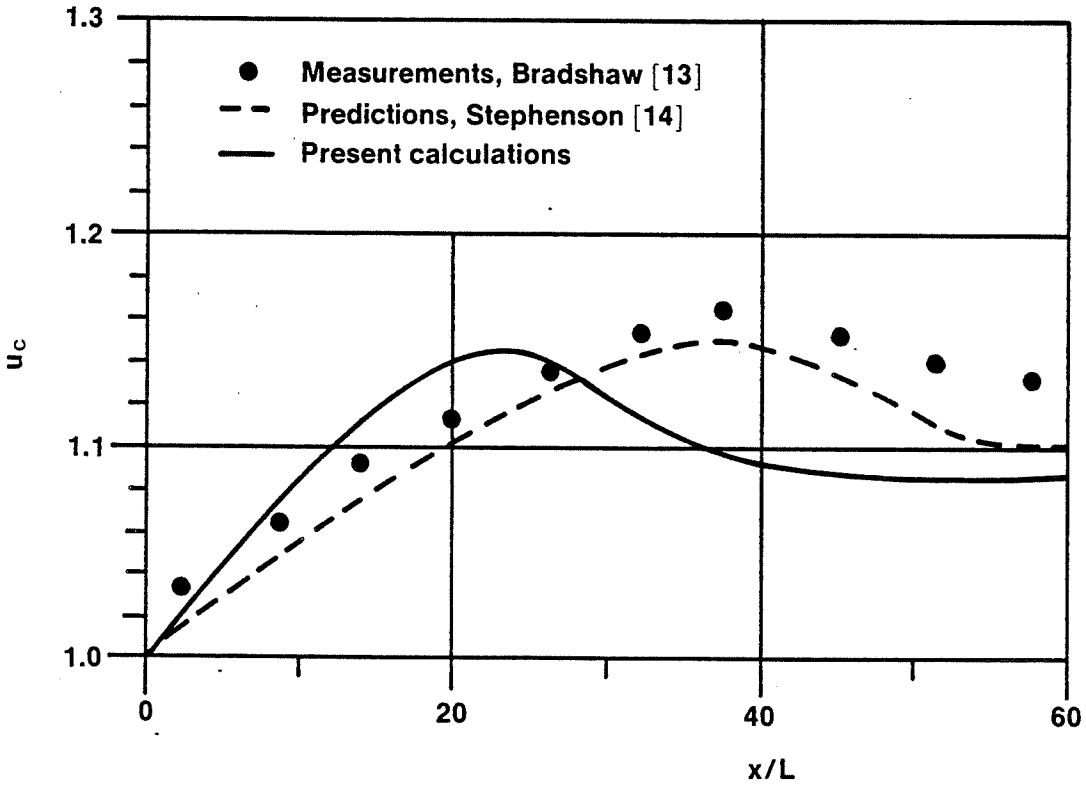
Measurements, Bradshaw [13]
Predictions, Stephenson [14]
Present calculations
1.3
1.2
1.1
1.0
u_c
0
20
40
60
x/L

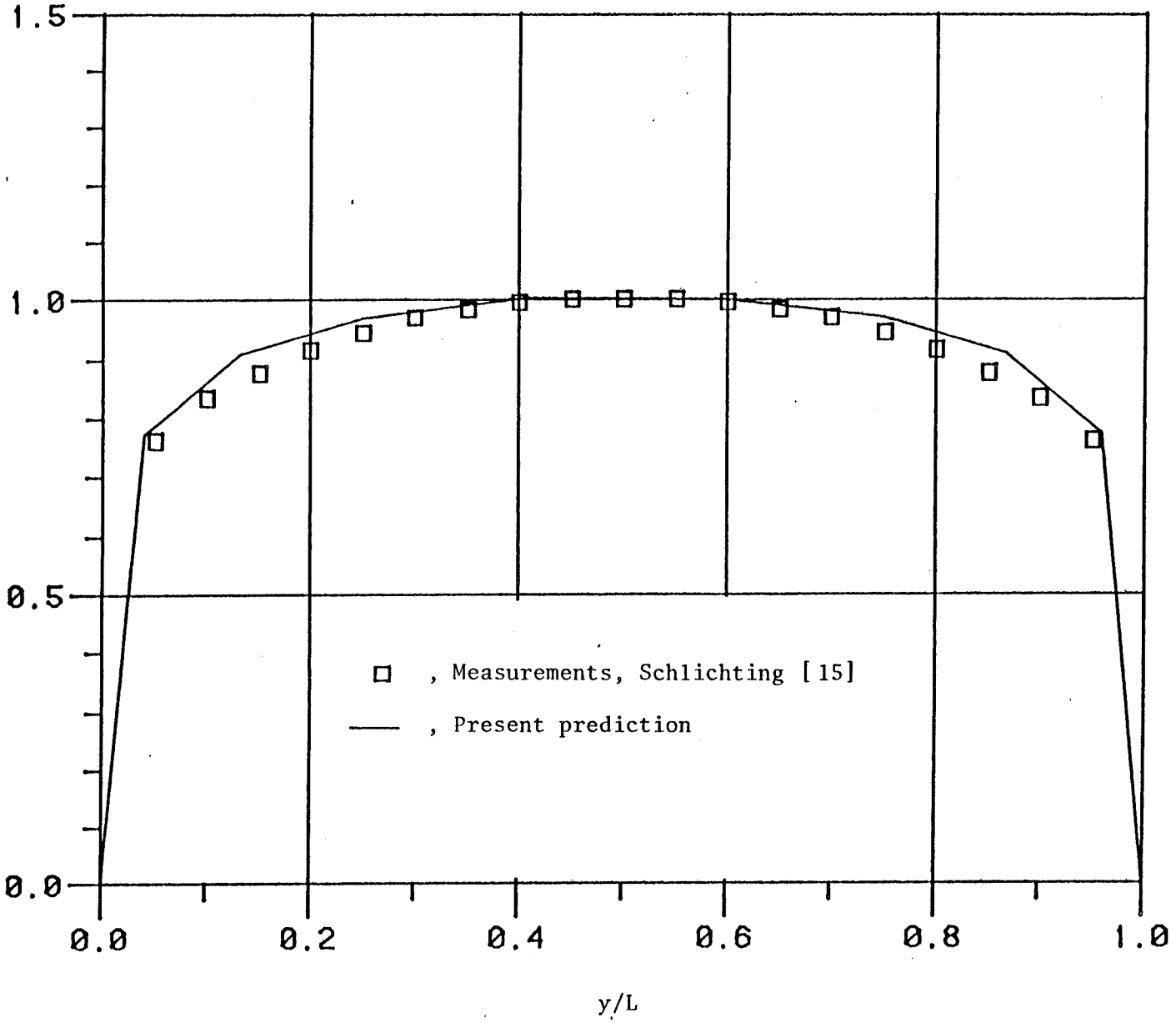
1.5
1.0
0.5
0.0
0.0
0.2
0.4
0.6
0.8
1.0
u/u_c
y/L
, Measurements, Schlichting [15]
, Present prediction

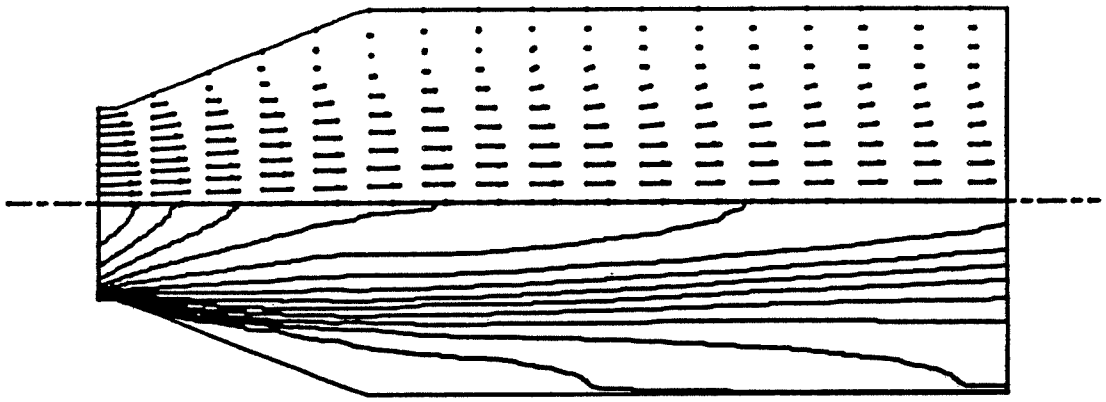

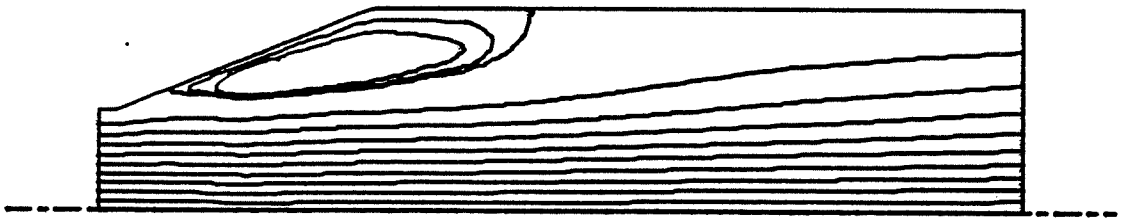

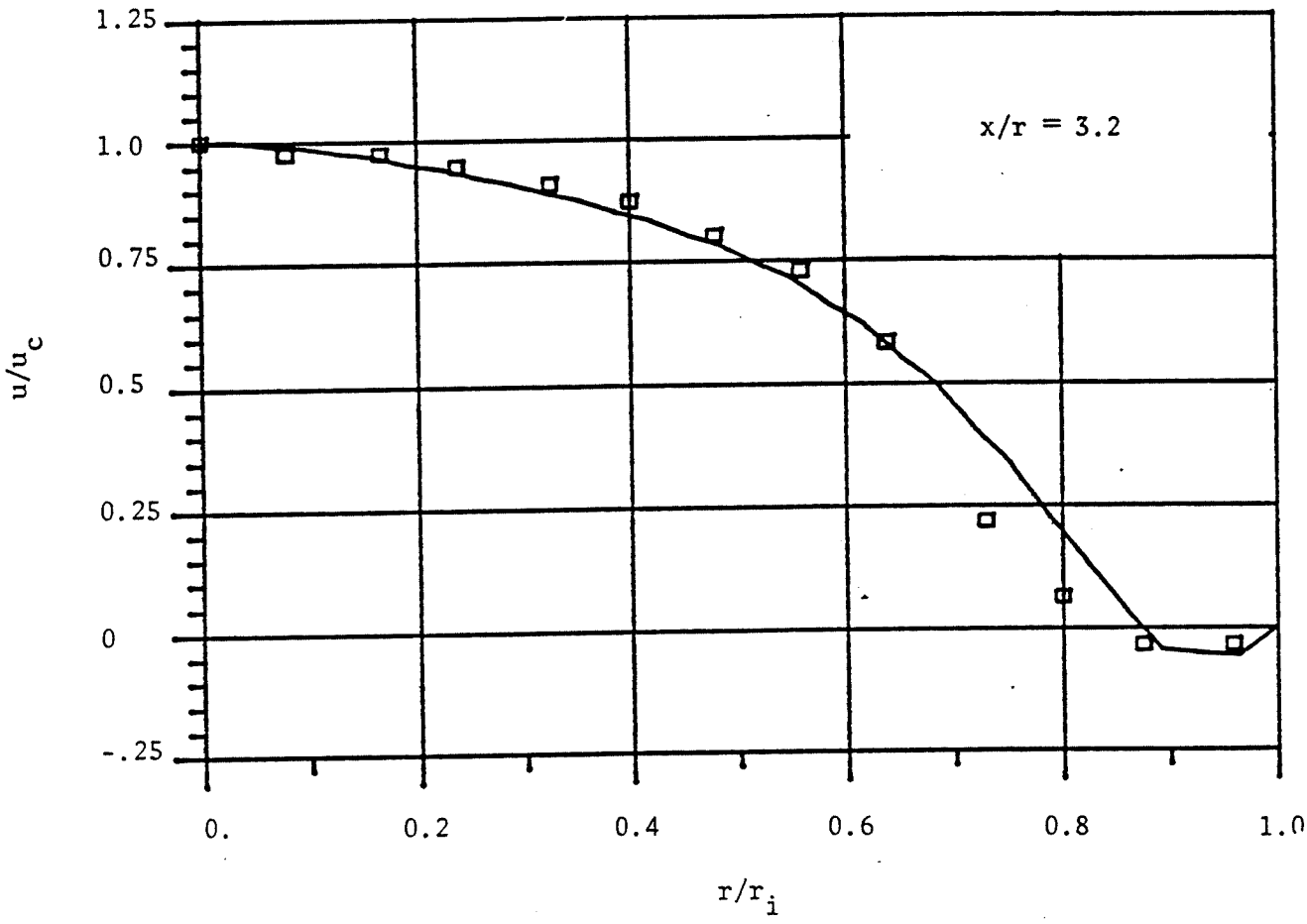
1.25
1.0
0.75
0.5
0.25
0
-.25
u/u_c
x/r = 3.2
0.
0.2
0.4
0.6
0.8
1.0
r/r_i

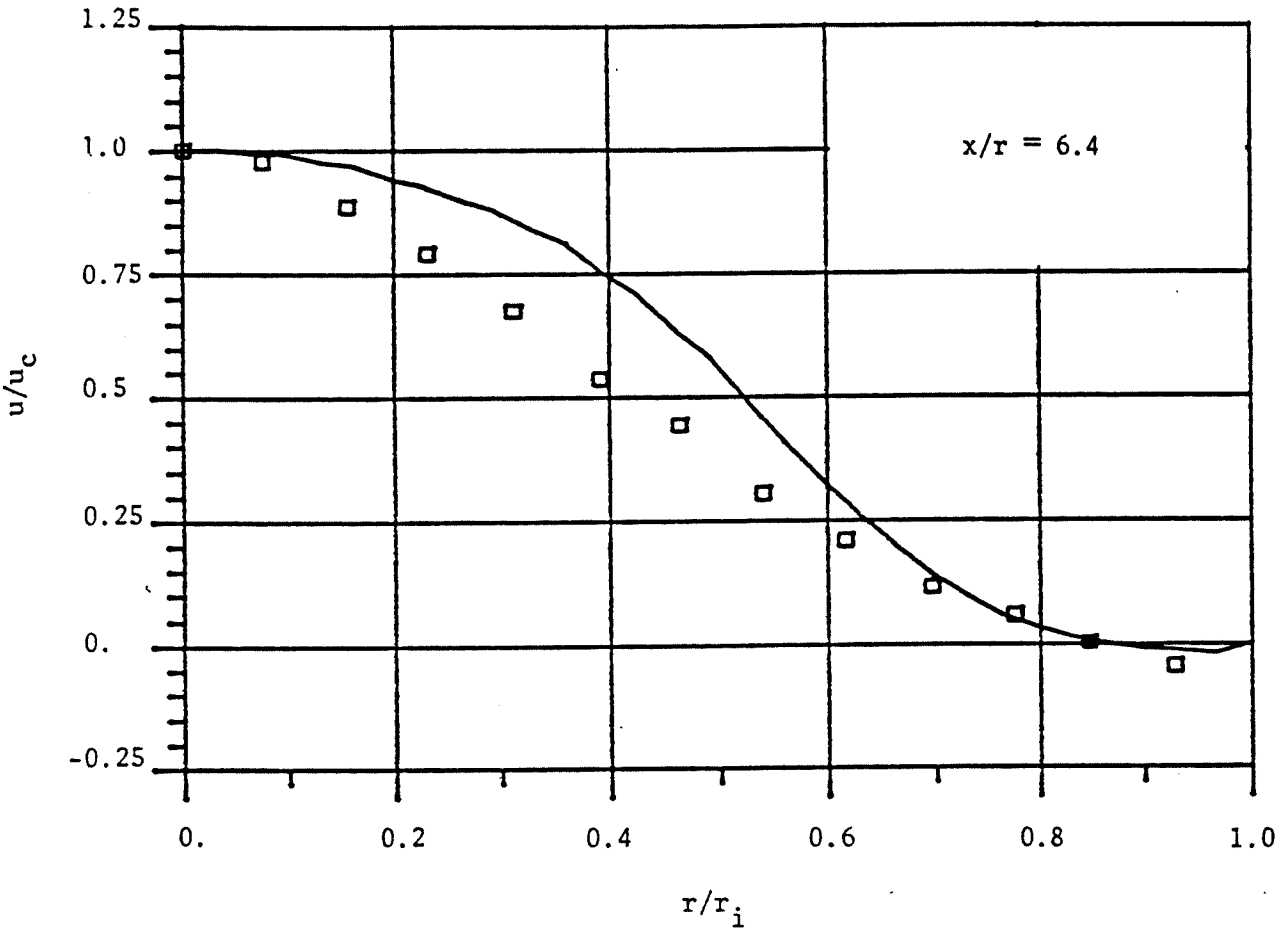
1.25
1.0
0.75
0.5
0.25
0.
-0.25
u/u_c
x/r = 6.4
0.
0.2
0.4
0.6
0.8
1.0
r/r_i

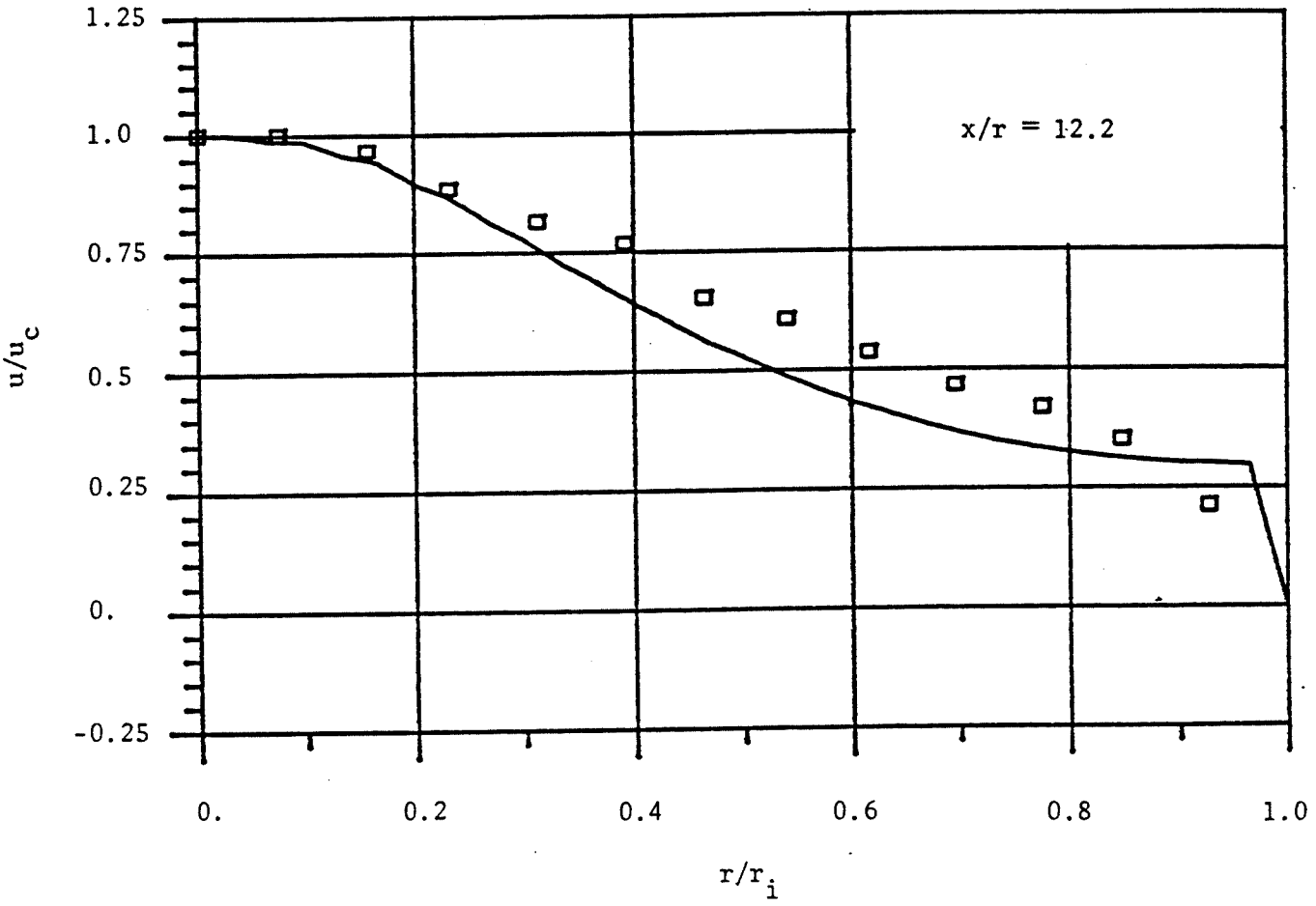
1.25
1.0
0.75
0.5
0.25
0.
-0.25
u/u_c
x/r = 12.2
0.
0.2
0.4
0.6
0.8
1.0
r/r_i

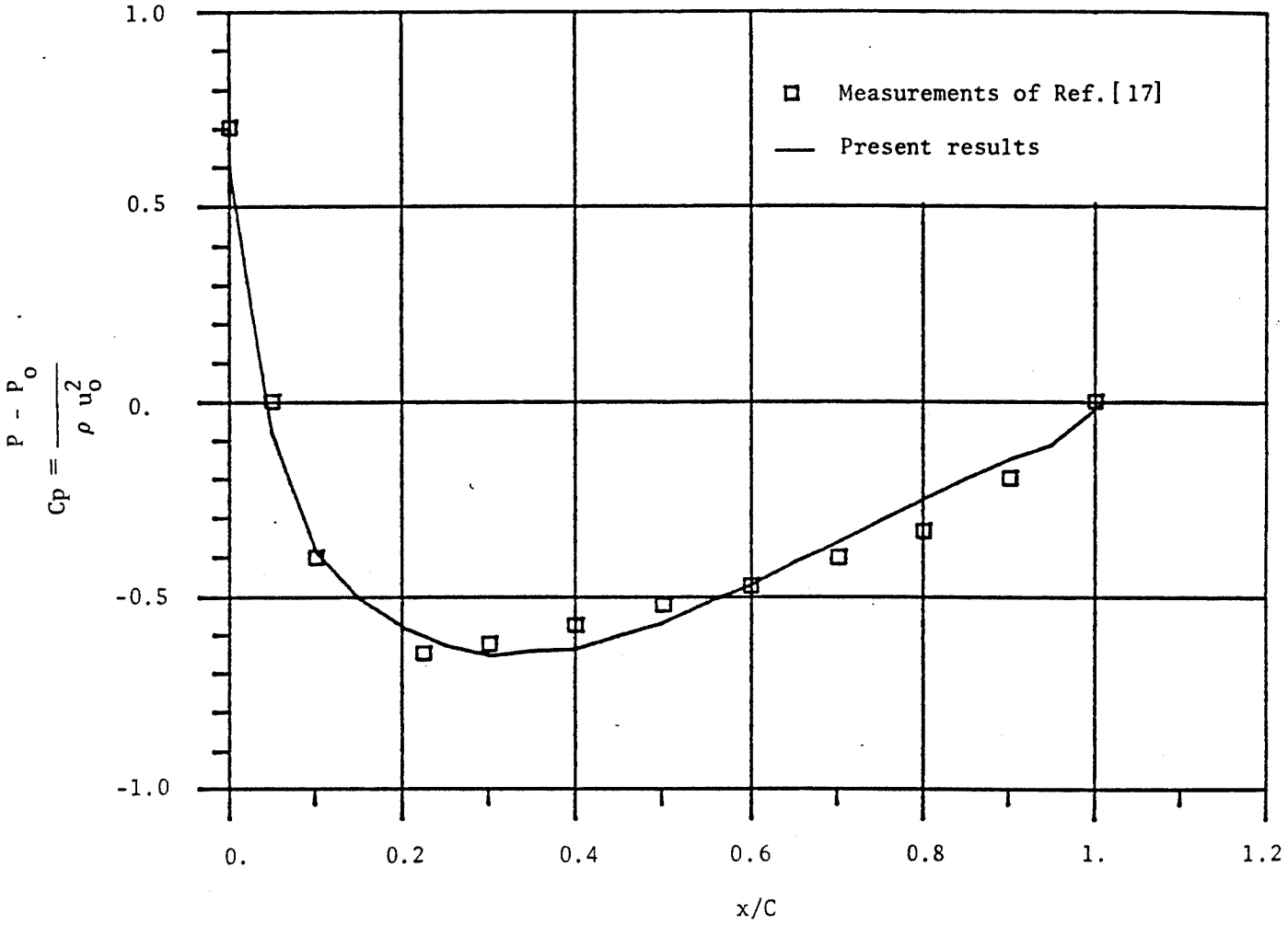
1.0
0.5
0.
-0.5
-1.0
0.
0.2
0.4
0.6
0.8
1.
1.2
x/C
$Cp = \frac{P - P_o}{\rho u_o^2}$
Measurements of Ref. [17]
Present results

LIST OF FIGURES

Figure